Eur. Phys. J. D **44**, 327–335 (2007)
DOI: 10.1140/epjd/e2007-00183-8

**THE EUROPEAN
PHYSICAL JOURNAL D**

Rydberg transitions for positron-hydrogen collisions

A. Ghoshal[1] and P. Mandal[2,a]

[1] Department of Mathematics, Burdwan University, Golapbag, Burdwan 713 104, West Bengal, India
[2] Department of Mathematics, Visva-Bharati University, Santiniketan 731 235, West Bengal, India

Received 19 January 2007 / Received in final form 19 April 2007

Abstract. $e^+ + \mathrm{H}(ns) \rightarrow e^+ + \mathrm{H}(n's)$ transitions for arbitrary n and n' have been studied using the distorted-wave formalism in the momentum space [1]. The distorted-wave scattering amplitudes have been written in a simple closed analytical form. A detailed study has been made on differential and total cross sections in the energy range 20–300 eV. Resonance-like behaviour of the differential cross section has been observed in the the region of lower scattering angles for high Rydberg transitions. To the best of our knowledge the distorted-wave results for differential and total cross sections for such arbitrary transitions are reported for the first time in the literature.

PACS. 34.60.+z Scattering in highly excited states (e.g., Rydberg states) – 34.85.+x Positron scattering

1 Introduction

Atomic transition processes involving arbitrary initial (nlm) and final ($n'l'm'$) states have found wide applications in many fields, such as, astrophysics, plasma physics etc. The knowledge of the differential cross sections of such processes are of utmost importance in order to interpret the distribution of emitted radiation. But in practice, sophisticated quantum mechanical treatment of such problems is too complicated to be carried out.

Though a number of perturbative and non-perturbative calculations [1–10] have been performed to study $1s-2s$ and $1s-2p$ excitations of hydrogen atom by positron impact, arbitrary excitation calculations have rarely been reported in the literature except using the first Born approximation (FBA) [11–14]. Sil and co-workers [12] reported closed form expressions for the FBA amplitude for $nlm - n'l'm'$ transitions in direct excitation and electron-capture processes during $e^{\pm} - \mathrm{H}$ and $p - \mathrm{H}$ collisions. The asymptotic form of the amplitude as $n \rightarrow \infty$ was also obtained. It was reported that the total cross section for all the processes satisfied (n^{-3})-law.

In this work, we have derived a general formula for obtaining the partial-wave distorted-wave amplitudes of positron-impact excitations to an arbitrary s-state from an arbitrary s-state of the hydrogen atom in closed analytical forms. Making use of these expressions, we have made a detailed study on the nature of the differential and total cross sections.

The distorted-wave theory in the momentum space as used in the paper was derived by the authors recently [1] by approximating the distortion potential in a particular channel as the average of perturbation of that particular channel over the bound states. The real advantage of this method is that a few straight forward calculations are required to compute the scattering amplitude in a closed analytical form for all partial waves. This theory was applied successfully to study $1s-2s$ excitation of hydrogen atom by positron impact and Ps(ns) ($n = 1, 2, 3$) formation in positron-hydrogen collisions in the intermediate and high energy range. The computed results of these processes compare nicely with other theoretical and experimental results available in the literature.

The plan of the paper is as follows. Presenting the details of our calculations in Section 2, we discuss our computed results in Section 3. Finally in Section 4 we make our concluding remarks.

2 Calculational details

We have used the distorted-wave amplitude in the momentum space as obtained previously [1]:

$$A_{fi}^{(L)}(k_f, k_i)] = g_B^{(L)}(k_f, k_i) + D_{fi}^{(L)}(k_f, k_i) \qquad (1)$$

where $g_B^{(L)}(k_f, k_i)$ and $D_{fi}^{(L)}(k_f, k_i)$ are obtained as:

$$[g_B^{(L)}(k_f, k_i)] = \frac{\sqrt{k_i k_f}}{2} \int_{-1}^{+1} [g_B(\vec{k_f}, \vec{k_i})] P_L(\cos\theta_f)\, d(\cos\theta_f),$$

and

$$[D_{fi}^{(L)}(k_f, k_i)] = \frac{\sqrt{k_i k_f}}{2} \int_{-1}^{+1} [D(\vec{k_f}, \vec{k_i})] P_L(\cos\theta_f)\, d(\cos\theta_f),$$

---

[a] e-mail: `puspajit2001@yahoo.com`

in which the two-body amplitudes are given by

$$g_B(\vec{k_f},\vec{k_i}) = \left(-\frac{2\pi}{\mu_f}\right)^{-1} \langle \Phi_f|V_f|\Phi_i\rangle;$$
$$f_{f\gamma}(\vec{k_f},\vec{k_i}) = \left(-\frac{2\pi}{\mu_\gamma}\right)^{-1} \langle \Phi_f|V_f|\Phi''_\gamma\rangle;$$
$$f_{\gamma i}(\vec{k_f},\vec{k_i}) = \left(-\frac{2\pi}{\mu_i}\right)^{-1} \langle \Phi''_\gamma|U_i|\Phi_i\rangle;$$

with the double scattering matrix elements

$$D_{fi}(\vec{k_f},\vec{k_i}) = \frac{1}{(2\pi)^3}\sum_\gamma \left(-\frac{2\pi}{\mu_\gamma}\right) \times \int \frac{d\vec{k''}}{E-E''_\gamma+i\epsilon} f_{f\gamma}(\vec{k_f},\vec{k_i}) f_{\gamma i}(\vec{k_f},\vec{k_i}). \quad (2)$$

Here γ denotes the intermediate states of hydrogen atom. The distorted-wave amplitude $A^{(L)}_{fi}(k_f,k_i)]$ is a function of the scattering energies for any partial wave L.

For $e^+ + \mathrm{H}(n00) \rightarrow e^+ + \mathrm{H}(n'00)$ collisions

$$U_i = \langle\phi_i|V_i|\phi_i\rangle = \langle\phi_{n00}|V_i|\phi_{n00}\rangle,$$
$$U_f = \langle\phi_f|V_f|\phi_f\rangle = \langle\phi_{n'00}|V_f|\phi_{n'00}\rangle,$$

where $V_i = (1/r_1 - 1/r_{12}) = V_f$, with the plane-wave states in the incident and the final channel are respectively given by

$$\Phi_i(\vec{r_1},\vec{r_2}) = e^{i\vec{k_i}.\vec{r}_1}\phi_i(\vec{r_2}) \quad \text{and} \quad \Phi_f(\vec{r_1},\vec{r_2}) = e^{i\vec{k_f}.\vec{r}_1}\phi_f(\vec{r_2})$$

in atomic units. $\phi_i(\vec{r_2})$, $\phi_f(\vec{r_2})$ are the wave functions of H-atom in the initial and the final channel respectively, where f corresponds to $(n'00)$, $n' = 1, 2, 3, ...$ and i corresponds to $(n00)$, $n = 1, 2, 3, ...$

Now the wave function of hydrogen atom in $n00$ state in atomic units is given by

$$\phi_{n00}(\vec{r}_2) = -\frac{1}{\sqrt{2\pi}}\frac{1}{\sqrt{2}}\left[\left(\frac{2}{n}\right)^3 \frac{(n-1)!}{2n(n!)^3}\right]^{\frac{1}{2}} e^{-\frac{r_2}{n}} L^1_n(\rho), \quad (3)$$

where $L^1_n(\rho)$ is the associated Laguerre polynomial of degree n with $\rho = 2r_2/n$. Using the relation between the associated Laguerre polynomial $L^p_q(\rho)$ and the Laguerre polynomial $L_q(\rho)$, $L^p_q(\rho) = d^pL_q(\rho)/d\rho^p$, and the Rodrigue formula for the Laguerre polynomial, $L_q(\rho) = e^\rho d^q(\rho^q\ e^{-\rho})/d\rho^q$, equation (3) can be written as

$$\phi_{n00}(\vec{r}_2) = -\frac{1}{\sqrt{2\pi}}\frac{1}{\sqrt{2}}\left[\left(\frac{2}{n}\right)^3 \frac{(n-1)!}{2n(n!)^3}\right]^{\frac{1}{2}} \times e^{-\frac{r_2}{n}} \frac{d}{d\rho}\left[e^\rho \frac{d^n}{d\rho^n}(\rho^p\ e^{-\rho})\right]. \quad (4)$$

Further, using Leibnitz's rule for successive derivative, equation (4) can be framed as

$$\phi_{n00}(\vec{r}_2) = -\frac{1}{\sqrt{2\pi}}\frac{1}{\sqrt{2}}\left[\left(\frac{2}{n}\right)^3 \frac{(n-1)!}{2n(n!)^3}\right]^{\frac{1}{2}} \times e^{-\frac{r_2}{n}} \sum_{t=1}^{n}(-1)^t\binom{n}{t}\frac{n!}{(t-1)!}\left(\frac{2}{n}\right)^{t-1} r_2^{t-1}$$

$$\text{or, } \phi_{n00}(\vec{r}_2) = -\frac{1}{4\sqrt{\pi}}\frac{1}{2}\left(\frac{2}{n}\right)^2\sqrt{\frac{1}{2}\left(\frac{2}{n}\right)} e^{-\frac{r_2}{n}} \times \sum_{t=1}^{n}(-1)^t\binom{n}{t}\frac{1}{(t-1)!}\left(\frac{2}{n}\right)^{t-1} r_2^{t-1}$$

$$\text{or, } \phi_{n00}(\vec{r}_2) = H(n)e^{-\frac{r_2}{n}}\sum_{t=1}^{n}(-1)^t\binom{n}{t}\frac{1}{(t-1)!}\left(\frac{2}{n}\right)^{t-1} r_2^{t-1} \quad (5)$$

with

$$H(n) = -\frac{1}{4\sqrt{\pi}}\frac{1}{2}\left(\frac{2}{n}\right)^2\sqrt{\frac{1}{2}\left(\frac{2}{n}\right)}.$$

The $n00-n'00$ inelastic amplitudes thus can be written as

$$\begin{aligned}
f_{fi}(\vec{k_f},\vec{k_i}) &= \left(-\frac{2\pi}{\mu_i}\right)^{-1}\langle\Phi_f|V_i|\Phi_i\rangle \\
&= \langle e^{i.\vec{k}_f.\vec{r}_1}\phi_{n'00}(\vec{r}_2)|V_i|e^{i.\vec{k}_i.\vec{r}_1}\phi_{n00}(\vec{r}_2)\rangle \\
&= \left(-\frac{2\pi}{\mu_i}\right)^{-1}\int e^{-i.\vec{k}_f.\vec{r}_2}\phi^*_{n'00}(\vec{r}_2)\ |V_i| \\
&\quad \times e^{i.\vec{k}_i.\vec{r}_1}\phi_{n00}(\vec{r}_2)\ d\vec{r}_1\ d\vec{r}_2 \\
&= \left(-\frac{2\pi}{\mu_i}\right)^{-1}[H(n')][H(n)] \\
&\quad \times \sum_{t=1}^{n}\ \sum_{s=1}^{n'}\ (-1)^{t+s}\binom{n}{t}\binom{n'}{s} \\
&\quad \times \frac{1}{(t-1)!(s-1)!}\left(\frac{2}{n}\right)^{t-1}\left(\frac{2}{n'}\right)^{s-1} \\
&\quad \times \int r_2^{t+s-2}e^{i.\vec{q}.\vec{r}_1-(\frac{1}{n}+\frac{1}{n'})r_2}\ V_i\ d\vec{r}_1\ d\vec{r}_2 \\
&= \left(-\frac{2\pi}{\mu_i}\right)^{-1}[H(n')][H(n)] \\
&\quad \times \sum_{t=1}^{n}\sum_{s=1}^{n'}\ (-1)^{t+s}\binom{n}{t}\binom{n'}{s} \\
&\quad \times \frac{1}{(t-1)!(s-1)!}\left(\frac{2}{n}\right)^{t-1}\left(\frac{2}{n'}\right)^{s-1} \\
&\quad \times EL(\vec{q},\frac{1}{n}+\frac{1}{n'},t+s-2), \qquad (6)
\end{aligned}$$

where $\vec{k}_i - \vec{k}_f = \vec{q}$ and

$$EL(\vec{q},b,n) = \int r_2^n e^{i.\vec{q}.\vec{r}_1 - br_2}\ V_i\ d\vec{r}_1\ d\vec{r}_2. \quad (7)$$

Taking Fourier integral transforms for functions of the form $\exp(-\lambda r)/r$, $\exp(-\lambda r)$:

$$\exp(-\lambda r)/r = \frac{1}{2\pi^2}\int \frac{e^{i\vec{p}.\vec{r}}}{p^2+\lambda^2}d\vec{p} \tag{8}$$

$$\exp(-\lambda r) = \frac{\lambda}{\pi^2}\int \frac{e^{i\vec{p}.\vec{r}}}{(p^2+\lambda^2)^2}d\vec{p} \tag{9}$$

and then utilising the δ-function properties, such as,

$$\begin{aligned}\int e^{i(\vec{q}-\vec{\Delta}).\vec{r}} f(\vec{q})d\vec{q}\; d\vec{r} &= (2\pi)^3 \int \delta(\vec{q}-\vec{\Delta})f(\vec{q})d\vec{q}\\ &= (2\pi)^3 f(\vec{\Delta}),\end{aligned} \tag{10}$$

we obtain

$$\begin{aligned}EL(\vec{q},b,0) &= \int e^{i.\vec{q}.\vec{r}_1 - br_2}\; V_i\; d\vec{r}_1\; d\vec{r}_2\\ &= 32\pi^2\left[\frac{1}{b^3(q^2+b^2)} - \frac{1}{2}\frac{-2b}{b^2(q^2+b^2)^2}\right].\end{aligned} \tag{11}$$

Utilising the formula of the nth order derivative of a function of the form $1/(a^2+x^2)$, such as,

$$\begin{aligned}DI(x,a,n) &= \frac{d^n}{dx^n}\left[\frac{1}{a^2+x^2}\right]\\ &= (-1)^n \frac{n!}{a}\frac{\sin\left[(n+1)\tan^{-1}\left(\frac{a}{x}\right)\right]}{(a^2+x^2)^{\frac{n+1}{2}}} \qquad \text{if } a \neq 0\\ &= (-1)^n\;\frac{(n+1)!}{x^{n+2}} \qquad \text{if } a = 0\end{aligned} \tag{12}$$

or

$$\frac{d^n}{dx^n}\left[\frac{1}{a^2+x^2}\right] = (-1)^n \sum_{r=0}^{R}(-1)^r \frac{\binom{n-r}{r}(2x)^{n-2r}}{(a^2+x^2)^{n+1-r}}$$
$$\begin{aligned}&\text{with } R = n/2 \text{ if } n \text{ is even,}\\ &\quad = (n-1)/2 \text{ if } n \text{ is odd}\end{aligned} \tag{13}$$

and Liebnitz's rule for successive differentiation, we obtain a closed form expression

$$\begin{aligned}EL(\vec{q},b,n) &= (-1)^n\frac{\partial^n}{\partial b^n}[EL(\vec{q},b,0)]\\ &= 16\pi^2\sum_{r=0}^{n}\;(-1)^r\binom{n}{r}\frac{(n-r+1)!}{b^{n-r+2}}\\ &\quad\times\left[(n-r+2)\frac{DI(b,q,r)}{b} - DI(b,q,r+1)\right].\end{aligned} \tag{14}$$

Substituting equation (13) in equation (6), we obtain the desired $n00 - n'00$ inelastic amplitudes.

From the above derivation it is evident that the scattering amplitudes in closed analytical forms are readily evaluated and easily interpreted.

3 Results and discussion

3.1 Differential cross section

In this paper, we have used the same theory as that of our previous paper [1] to calculate and verify the differential cross section. In our previous work [1] we compared our results of differential cross section for $1s-2s$ excitation of hydrogen atom by positron impact with other theoretical predictions [4–7] and showed that our findings are in nice agreement with those theoretical results. Further, it was found that the differential cross section for $1s-2s$ transition in positron-hydrogen collisions did not show any interesting feature. It simply behaves like a monotonic decreasing function of the scattering angle, which falls down sharply from the forward angles. However, the differential cross section for higher order transitions in positron-hydrogen collisions present some dramatic behaviour.

We present our results for differential cross sections for the $2s-3s, 3s-4s$ and $4s-5s$ in Table 1 at some discrete angles. It is clear from this table that the differential cross section is highly peaked at 0° and this peak rises up with increasing n. Further the peak falls down as the difference of n' and n increases. It is worthwhile to mention here that the very high cross sections at the forward scattering angles negligibly contribute to the total cross section because of the presence of the factor $\sin\theta$ in the formula, $\sigma_t = 2\int_0^\pi (d\sigma/d\Omega)\sin\theta\; d\theta$. The main reason for large differential cross sections at 0° is as follows.

The energy conservation for ns to $n's$ excitation of hydrogen by positron impact in a.u. is given by

$$k_i^2 - k_f^2 = \left(\frac{1}{n^2} - \frac{1}{n'^2}\right), \tag{15}$$

where k_i and k_f are the momenta of the incident and scattered positron respectively. Now as the value of the expression in the right hand side of equation (15) decreases k_i becomes close to k_f and consequently the contribution of Born's amplitude increases indefinitely at 0°. Moreover the rapid increase of the differential cross section with higher values of n follows the Rutherford scattering formula [15] which predicts infinite cross section at 0° and thus our results for scattering cross section seem to be in accordance with the correspondence principle.

It is clear from the Table 1 that, though for $1s-2s$ and $2s-3s$ transitions, the differential cross sections decrease steadily with higher scattering angles, appreciable variation in differential cross section with varying scattering angle is observed for $3s-4s$ and higher transitions. The amount and nature of variation in differential cross section for different transitions are controlled by the quantity $k_i^2 - k_f^2$. Our findings indicate that the lesser the value of $k_i^2 - k_f^2$, the greater the variation in differential cross section. It has been found that whenever $k_i^2 - k_f^2 > 0.1$ a.u. (approx.) no variation in differential cross section occur with varying scattering angles.

Variation of the differential cross sections at the forward scattering angles for transition from the higher states

Table 1. Inelastic differential cross sections of the atomic hydrogen by positron impact, in a.u. σ^t denote the total cross section in units of πa_0^2. The notation $x[-y]$ stands for $x \times 10^{-y}$.

	Angle	Energy (eV)				
Transitions	(deg)	40.0	50.0	60.0	150.0	250.0
$2s \to 3s$	0	0.9893[+02]	0.9903[+02]	0.9910[+02]	0.9927[+02]	0.9927[+02]
	5	0.6625[+02]	0.5970[+02]	0.5379[+02]	0.2131[+02]	0.7813[+01]
	10	0.2129[+02]	0.1443[+02]	0.9844[+01]	0.4685[+00]	0.7539[−01]
	30	0.2055[+00]	0.1050[+00]	0.6018[−01]	0.4608[−02]	0.1312[−02]
	45	0.4222[−01]	0.2171[−01]	0.1272[−01]	0.9041[−03]	0.2347[−03]
	60	0.1493[−01]	0.7736[−02]	0.4480[−02]	0.2133[−03]	0.2417[−04]
	90	0.3864[−02]	0.1946[−02]	0.1111[−02]	0.8440[−04]	0.2728[−04]
	120	0.1684[−02]	0.8357[−03]	0.4697[−03]	0.1863[−04]	0.1174[−05]
	150	0.1073[−02]	0.5356[−03]	0.3061[−03]	0.2856[−04]	0.1199[−04]
	180	0.9232[−03]	0.4497[−03]	0.2422[−03]	0.3385[−05]	0.3588[−04]
	σ^t	0.2120[+01]	0.1638[+01]	0.1326[+01]	0.4094[+00]	0.1802[+00]
$3s \to 4s$	0	0.1744[+04]	0.1727[+04]	0.1716[+04]	0.1685[+04]	0.1679[+04]
	5	0.3827[+03]	0.2538[+03]	0.1683[+03]	0.3812[+01]	0.1098[+00]
	10	0.1677[+02]	0.9551[+01]	0.6291[+01]	0.5246[+00]	0.2975[−01]
	30	0.2682[+00]	0.1563[+00]	0.1014[+00]	0.7103[−02]	0.3627[−03]
	45	0.4806[−01]	0.2859[−01]	0.1903[−01]	0.1347[−02]	0.6245[−04]
	60	0.8643[−02]	0.3198[−02]	0.1275[−02]	0.7235[−06]	0.4678[−07]
	90	0.5610[−02]	0.3571[−02]	0.2485[−02]	0.2049[−03]	0.9501[−05]
	120	0.6768[−03]	0.1678[−03]	0.3371[−04]	0.6642[−05]	0.3196[−06]
	150	0.2144[−02]	0.1545[−02]	0.1182[−02]	0.1257[−03]	0.5802[−05]
	180	0.2269[−02]	0.4418[−02]	0.5511[−02]	0.1369[−02]	0.6330[−04]
	σ^t	0.7569[+01]	0.5235[+01]	0.3813[+01]	0.4047[+00]	0.2526[−01]
$4s \to 5s$	0	0.1358[+05]	0.1344[+05]	0.1335[+05]	0.1324[+05]	0.1327[+05]
	5	0.2402[+03]	0.8530[+02]	0.3126[+02]	0.5392[+00]	0.1625[+00]
	10	0.3315[+02]	0.1592[+02]	0.7123[+01]	0.2950[−02]	0.5879[−02]
	30	0.4961[+00]	0.2228[+00]	0.9555[−01]	0.1928[−04]	0.6222[−04]
	45	0.9216[−01]	0.4181[−01]	0.1808[−01]	0.3060[−05]	0.1067[−04]
	60	0.7950[−04]	0.1231[−04]	0.8575[−05]	0.6302[−06]	0.2476[−07]
	90	0.1453[−01]	0.6699[−02]	0.2898[−02]	0.9660[−06]	0.1577[−05]
	120	0.3783[−03]	0.2479[−03]	0.1182[−03]	0.2046[−06]	0.3663[−07]
	150	0.8785[−02]	0.4142[−02]	0.1802[−02]	0.7558[−06]	0.9388[−06]
	180	0.9204[−01]	0.4630[−01]	0.2052[−01]	0.1272[−04]	0.9572[−05]
	σ^t	0.1101[+02]	0.5476[+01]	0.2575[+01]	0.2267[−02]	0.4473[−02]

of hydrogen atom, such as $5s$, $6s$, $10s$ etc., to the next higher states is of particular importance. To have a transparent idea about such a variation we have plotted the differential cross sections for $5s-6s$, $6s-7s$ and $10s-11s$ transitions as a function of scattering angle in the range 0°–10° in Figures 1a–1c.

In each case, the differential cross section first falls abruptly from its peak value at 0° to the primary minimum[1], and then rises to a secondary maxima. It then again falls down to a secondary minimum nearly equal to the primary minimum and then rises up to a secondary maxima which is much above the first secondary maxima and is the second global maximum. It is to be mentioned here that the formation of second secondary minimum and secondary maximum depends on the factor $k_i^2 - k_f^2$. Whenever there is a variation in differential cross section, the primary minimum and the first secondary maximum are formed first, subsequently other maxima and minima are formed depending on the factor $k_i^2 - k_f^2$. For instance, in case of $5s$ to $8s$ transition, only the primary minimum and the first secondary maximum are observed for 50 eV of energy but as the energy increases the first secondary minimum along with second secondary start forming. With the higher values of n or energy, these maxima and minima slowly move towards the forward direction and more maxima and minima of comparatively less values start forming from the backward direction. Further the value of the second global maximum increases with higher values of n. But beyond the scattering angle of 10° the differential cross section assumes nearly zero value, though there is a little regular variation beyond this scattering angle, it is not very much appreciable. The surface plots in Figures 2 and 3 make this nature of the differential cross section more transparent.

---

[1] We call the first local maximum and minimum of the differential cross section near the forward direction as the primary maximum and minimum respectively. The other local maxima and minima are called secondary maxima and minima respectively.

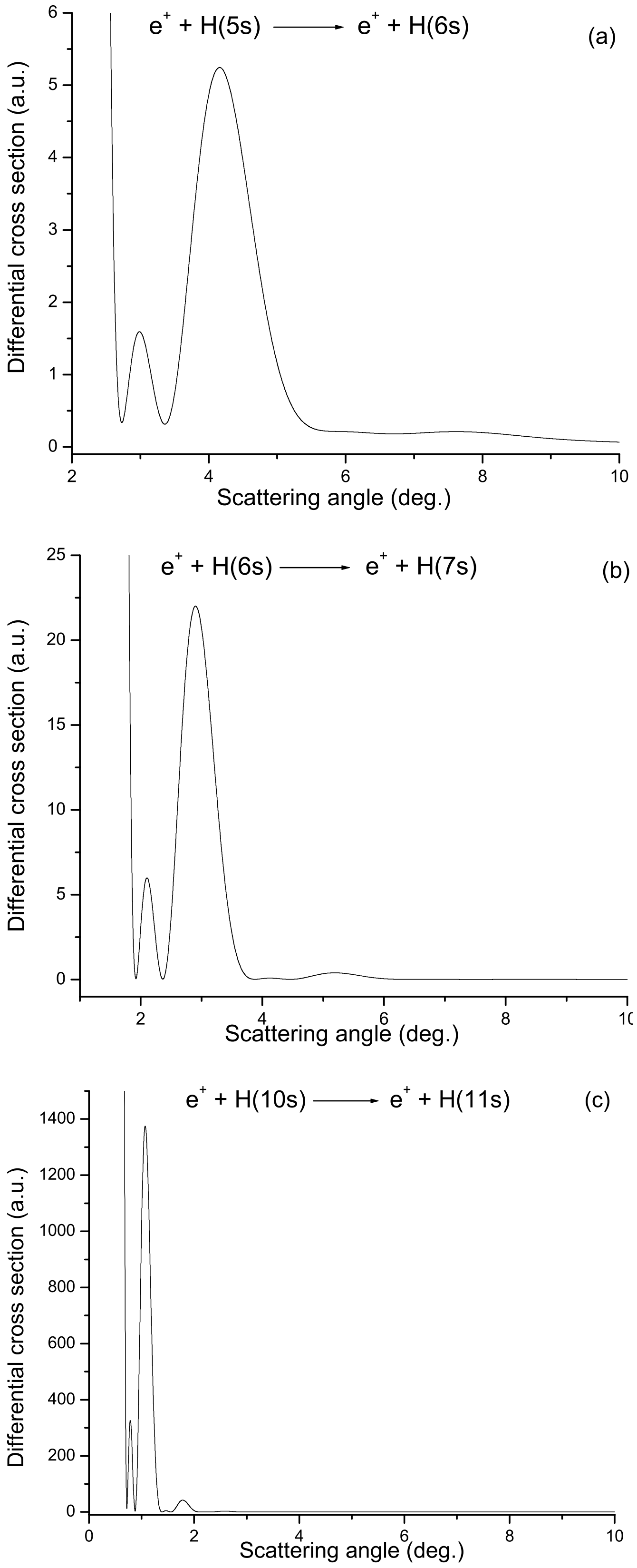

Fig. 1. Differential cross section (a.u.) as a function of scattering angle (deg) for (a) $e^+ + \mathrm{H}(5s) \rightarrow e^+ + \mathrm{H}(6s)$, (b) $e^+ + \mathrm{H}(6s) \rightarrow e^+ + \mathrm{H}(7s)$ and (c) $e^+ + \mathrm{H}(10s) \rightarrow e^+ + \mathrm{H}(11s)$ transitions at 100 eV of incident positron energy.

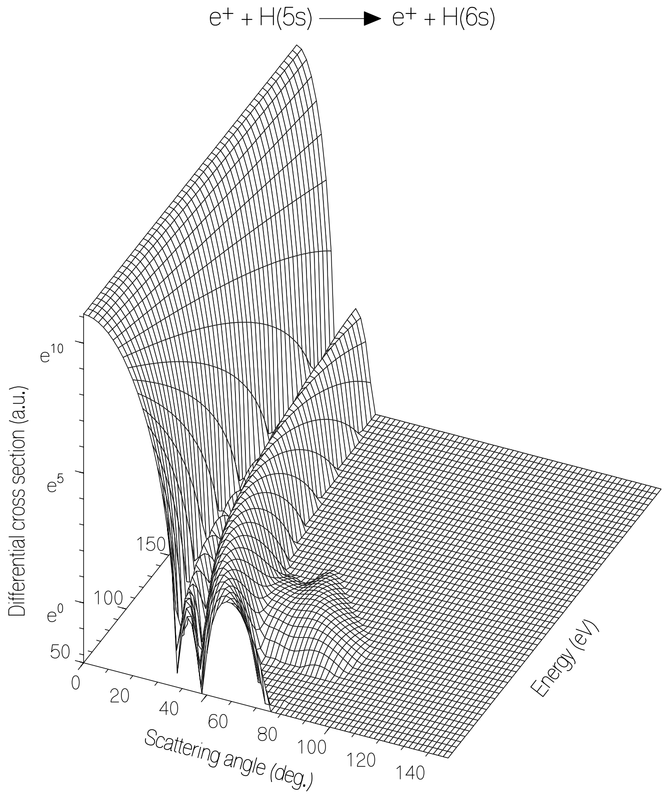

Fig. 2. Differential cross section (a.u.) as a function of energy (50–300 eV) and scattering angle (0°–15°) for the transition $e^+ + \mathrm{H}(5s) \rightarrow e^+ + \mathrm{H}(6s)$. The angles in the figures have been magnified by 10 units.

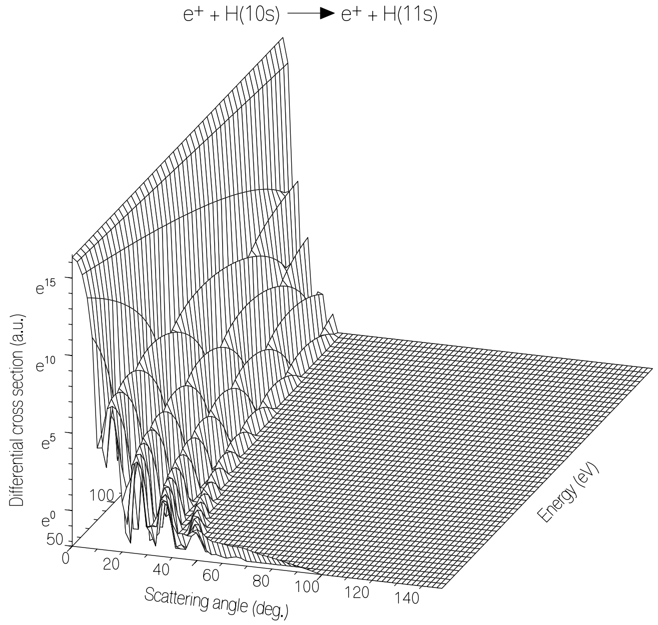

Fig. 3. Differential cross section (a.u.) as a function of energy (50–300 eV) and scattering angle (0°–15°) for the transition $e^+ + \mathrm{H}(5s) \rightarrow e^+ + \mathrm{H}(6s)$. The angles in the figures have been magnified by 10 units.

Table 2. Movement of the primary minimum (θ_p) and second global maximum (θ_s) with energy along with the corresponding differential cross sections $[d\sigma/d\Omega]_{\theta_p}$ and $[d\sigma/d\Omega]_{\theta_s}$ in a.u. respectively.

Energy (eV)		50.0	60.0	75.0	100.0	150.0	200.0	250.0
$5s-6s$	θ_p	3.8400	3.5000	3.1400	2.7300	2.2300	1.9300	1.7200
	$\left[\frac{d\sigma}{d\Omega}\right]_{\theta_p}$	0.0635	0.1728	0.0025	0.3332	0.1969	0.0095	0.0032
	θ_s	5.8900	5.3700	4.8100	4.1600	3.400	2.9400	2.6300
	$\left[\frac{d\sigma}{d\Omega}\right]_{\theta_s}$	4.4493	4.3396	4.5160	5.2456	5.1091	4.8107	4.8020
$5s-7s$	θ_p	4.3800	3.9300	3.5100	3.0600	2.5000	2.1600	1.9300
	$\left[\frac{d\sigma}{d\Omega}\right]_{\theta_p}$	3.4190	0.1290	0.0233	0.0172	0.1217	0.0166	0.0004
	θ_s	6.2600	5.800	5.1900	4.4900	3.6700	3.1800	2.8400
	$\left[\frac{d\sigma}{d\Omega}\right]_{\theta_s}$	4.4290	1.7643	1.6314	1.8469	2.0304	1.8627	1.8337
$5s-8s$	θ_p	5.6000	4.2200	3.7400	3.2500	2.6600	2.3000	2.0600
	$\left[\frac{d\sigma}{d\Omega}\right]_{\theta_p}$	4.4356	0.6670	0.0007	0.0001	0.0631	0.0174	0.0006
	θ_s	×	6.0300	5.4300	4.7000	3.8300	3.3200	2.9700
	$\left[\frac{d\sigma}{d\Omega}\right]_{\theta_s}$	×	1.4103	0.80158	0.8851	1.0315	0.9504	0.9211
$6s-7s$	θ_p	2.7300	2.4900	2.2200	1.9200	1.5700	1.3600	1.2200
	$\left[\frac{d\sigma}{d\Omega}\right]_{\theta_p}$	3.0315	3.6220	1.5036	0.0248	0.0061	0.0245	0.0532
	θ_s	4.1000	3.7400	3.3500	2.9000	2.3700	2.0500	1.8300
	$\left[\frac{d\sigma}{d\Omega}\right]_{\theta_s}$	26.1668	26.8157	24.0336	22.0133	22.3909	22.3842	22.2656
$6s-8s$	θ_p	3.0900	2.8300	2.5300	2.1900	1.7900	1.5500	1.3800
	$\left[\frac{d\sigma}{d\Omega}\right]_{\theta_p}$	0.0750	0.7909	1.0984	0.1306	0.0063	0.0168	0.0095
	θ_s	4.4900	4.1000	3.6600	3.1700	2.5900	2.2400	2.0100
	$\left[\frac{d\sigma}{d\Omega}\right]_{\theta_s}$	8.3319	9.5578	9.7114	8.3294	8.3109	8.3570	8.2976
$7s-8s$	θ_p	2.0200	1.8400	1.6500	1.4300	1.1700	1.0100	0.9000
	$\left[\frac{d\sigma}{d\Omega}\right]_{\theta_p}$	0.8570	0.0821	0.0102	0.2256	0.0727	0.0085	0.2424
	θ_s	3.0300	2.7700	2.4800	2.1400	1.7500	1.5200	1.3600
	$\left[\frac{d\sigma}{d\Omega}\right]_{\theta_s}$	78.3090	77.5414	79.1160	79.4364	78.6471	78.8859	78.7945
$7s-9s$	θ_p	2.3300	2.1200	1.9000	1.6500	1.3400	1.1600	1.0400
	$\left[\frac{d\sigma}{d\Omega}\right]_{\theta_p}$	2.6536	0.1098	0.0134	0.1074	0.0397	0.0567	0.0091
	θ_s	3.3500	3.0600	2.7400	2.3700	1.9400	1.6800	1.5000
	$\left[\frac{d\sigma}{d\Omega}\right]_{\theta_s}$	31.2350	27.8930	28.3892	28.9971	28.4549	28.6115	28.5960

× denotes the non-existence of the corresponding quantity.

What we proved in our previous paper [1] as the reasons for formation of maxima and minima in the differential cross section for positronium formation in positron-hydrogen collisions have been found to be true for inelastic positron-hydrogen collisions as well. A minimum in the differential cross section is formed due to destructive interference of the scattered waves of different angular momentum states where as a maximum is formed due to the constructive interference of the scattered waves of different angular momentum states. Actually the behaviour of sudden rise and fall of the differential cross section within a very short range of scattering angle, particularly for ns to $(n+1)s$ higher order transitions, where the sizes of rise and fall are substantial, is definitely a resonance-like charateristic of the differential cross section. We list in Table 2 the movement of primary minimum and second global maximum with increasing energy along with their corresponding differential cross sections in order to get a clear insight of the fact.

It is by now established by our previous studies [1,16,17] on elastic positron collisions and positronium formation that diffraction oscillations of the differential cross section due to interference of partial waves give rise to the presence of maxima and minima at the critical angles for low and intermediate energies of positron impact.

In the present study it is reported for the first time that orbiting oscillations do occur for positron-impact excitation processes, $n \geq 5$. The signature of orbiting of the positron around the target is apparent with the appearance of pronounced resonance-like structure in the corresponding differential cross section. We have displayed this nature in Figures 1a–1c for $5s-6s$, $6s-7s$ and $10s-11s$ transitions respectively at the energies 50 eV, 100 eV, 150 eV; the relevant resonance profiles are enlisted in Table 3 for $8s-9s$, $9s-10s$ and $10s-11s$ transitions at some discrete energies. It is evident from the table that the half-width decreases with the increasing energy as well as the higher order of transition. To the best of our knowledge this behaviour of the differential cross section for positron-impact excitations has not been reported so far.

However, for elastic atom-atom collisions, the effect of orbiting on the differential and total cross sections has been very well studied both theoretically [18–21] and

Table 3. Resonance profile – resonance angle (θ_r) (in deg.) along with the corresponding differential cross section $[d\sigma/d\Omega]_{\theta_s}$ (in a.u.) and half width $\Gamma/2$ (in deg). The resonance angle corresponds to the second global maximum (θ_s). The notation $x[y]$ stands for $x \times 10^y$.

Energy (eV)		50.0	75.0	100.0	150.0	200.0	250.0
	θ_r	2.34	1.91	1.65	1.35	1.17	1.04
$8s-9s$	$\left[\frac{d\sigma}{d\Omega}\right]_{\theta_r}$	0.2367[3]	0.2303[3]	0.2323[3]	0.2315[3]	0.2318[3]	0.2316[3]
	$\Gamma/2$	0.22	0.18	0.15	0.12	0.11	0.09
	θ_r	1.86	1.52	1.31	1.07	0.93	0.83
$9s-10s$	$\left[\frac{d\sigma}{d\Omega}\right]_{\theta_r}$	0.5928[3]	0.5954[3]	0.5948[3]	0.5953[3]	0.5952[3]	0.5955[3]
	$\Gamma/2$	0.17	0.14	0.12	0.09	0.08	0.07
	θ_r	1.51	1.23	1.07	0.87	0.76	0.68
$10s-11s$	$\left[\frac{d\sigma}{d\Omega}\right]_{\theta_r}$	0.1375[4]	0.1380[4]	0.1377[4]	0.1378[4]	0.1376[4]	0.1375[4]
	$\Gamma/2$	0.13	0.11	0.10	0.07	0.07	0.06

Table 4. Integrated cross section for $e^+ + \mathrm{H}(ns) \rightarrow e^+\mathrm{H}(n's)$, in units of πa_0^2. The notation $x[-y]$ stands for $x \times 10^{-y}$.

Energy (eV)	20	54.4	75	100	200	300
$1s-2s$	0.2852[+00]	0.1135[+00]	0.8206[−01]	0.6133[−01]	0.3044[−01]	0.2018[−01]
$1s-3s$	0.5641[−01]	0.2294[−01]	0.1652[−01]	0.1231[−01]	0.6080[−02]	0.4034[−02]
$1s-4s$	0.2082[−01]	0.8581[−02]	0.6172[−02]	0.4594[−02]	0.2264[−02]	0.1502[−02]
$1s-5s$	0.1003[−01]	0.4163[−02]	0.2993[−02]	0.2226[−02]	0.1097[−02]	0.7270[−03]
$1s-8s$	0.2293[−02]	0.9602[−03]	0.6899[−03]	0.5129[−03]	0.2524[−03]	0.1673[−03]
$1s-10s$	0.1156[−02]	0.4853[−03]	0.3486[−03]	0.2592[−03]	0.1275[−03]	0.8449[−04]
$1s-15s$	0.3375[−03]	0.1420[−03]	0.1020[−03]	0.7580[−04]	0.3728[−04]	0.2470[−04]
$2s-3s$	0.4876[+01]	0.1486[+01]	0.1018[+01]	0.7125[+00]	0.2633[+00]	0.1280[+00]
$2s-4s$	0.1032[+01]	0.3031[+00]	0.2101[+00]	0.1505[+00]	0.6261[−01]	0.3502[−01]
$2s-5s$	0.4061[+00]	0.1169[+00]	0.8095[−01]	0.5824[−01]	0.2479[−01]	0.1445[−01]
$2s-8s$	0.7665[−01]	0.2163[−01]	0.1493[−01]	0.1077[−01]	0.4641[−02]	0.2783[−02]
$2s-10s$	0.3711[−01]	0.1043[−01]	0.7191[−02]	0.5187[−02]	0.2240[−02]	0.1349[−02]
$2s-15s$	0.1042[−01]	0.2915[−02]	0.2008[−02]	0.1449[−02]	0.6266[−03]	0.3786[−03]
$3s-4s$	0.2148[+02]	0.4531[+01]	0.2514[+01]	0.1350[+01]	0.1104[+00]	0.4206[−02]
$3s-5s$	0.4550[+01]	0.1085[+01]	0.6837[+00]	0.4455[+00]	0.7537[−01]	0.6487[−02]
$3s-6s$	0.1788[+01]	0.4293[+00]	0.2754[+00]	0.1910[+00]	0.4549[−01]	0.5513[−02]
$3s-8s$	0.5379[+00]	0.1289[+00]	0.8203[−01]	0.5865[−01]	0.1878[−01]	0.3074[−02]
$3s-10s'$	0.2386[+00]	0.5715[−01]	0.3604[−01]	0.2587[−01]	0.9345[−02]	0.1739[−02]
$4s-5s$	0.4786[+02]	0.3962[+01]	0.7138[+00]	0.4148[−01]	0.2522[−03]	0.6111[−02]
$4s-6s$	0.1148[+02]	0.2186[+01]	0.7065[+00]	0.1127[+00]	0.2093[−03]	0.2108[−02]
$4s-7s$	0.4576[+01]	0.1123[+01]	0.4808[+00]	0.1121[+00]	0.2412[−03]	0.8016[−03]
$4s-9s$	0.1415[+01]	0.3845[+00]	0.2137[+00]	0.6928[−01]	0.7077[−04]	0.1696[−03]
$5s-6s$	0.5948[+02]	0.5762[−02]	0.1084[−02]	0.3199[−01]	0.1023[−02]	0.5079[−05]
$5s-7s$	0.2561[+02]	0.6741[−01]	0.3389[−02]	0.1593[−02]	0.2345[−02]	0.1217[−04]
$5s-9s$	0.5543[+01]	0.1907[+00]	0.1446[−02]	0.4434[−03]	0.2200[−02]	0.6315[−05]
$6s-7s$	0.3899[+01]	0.2296[+00]	0.1030[+00]	0.1647[−02]	0.3211[−02]	0.1205[−05]
$6s-8s$	0.1262[+02]	0.2267[−01]	0.7997[−01]	0.9719[−02]	0.1768[−02]	0.1437[−04]
$6s-9s$	0.1222[+02]	0.3496[−03]	0.4066[−01]	0.1392[−01]	0.8995[−03]	0.3135[−04]
$10s-11s$	0.5584[+00]	0.1016[−01]	0.4621[−03]	0.1065[−02]	0.6767[−05]	0.4106[−04]

experimentally [22,23]. For these systems the theoretical extensive studies have been made possible by the use of semi-classical and Regge-pole methods due to the heavy-particle nature of collisions which may not be readily applicable to the purely quantum collision systems involving electrons and positrons with atoms and molecules as in the present case.

Detailed study on the nature of orbiting around the target and the formation of temporary bound states are of very importance for collisional studies in atomic, molecular and nuclear physics and chemistry in particular. They require a separate and special treatment. Methods particularly suited for these studies, such as, the complex rotation or the R-matrix method [24] should be employed for accurate determination of the angle and life-time (width) of the Lorenz profile.

Thus a comprehensive study seems to have been made on arbitrary inelastic differential cross section for positron-hydrogen collisions at intermediate and high energies. Our

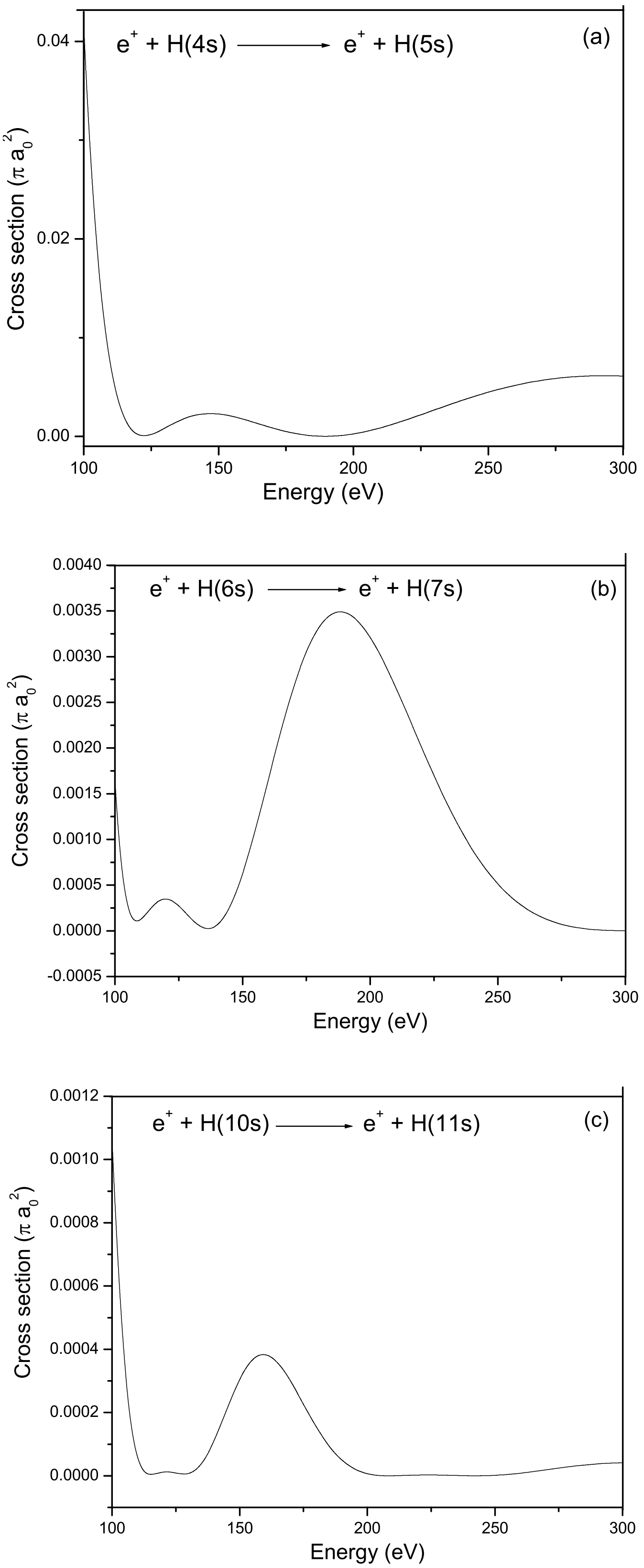

Fig. 4. Total cross section ($\pi\ a_0^2$) for (a) $e^+ + \mathrm{H}(4s) \rightarrow e^+ + \mathrm{H}(5s)$, (b) $e^+ + \mathrm{H}(6s) \rightarrow e^+ + \mathrm{H}(7s)$ and (c) $e^+ + \mathrm{H}(10s) \rightarrow e^+ + \mathrm{H}(11s)$ transitions in the range 100–300 eV.

investigations reveal the following important information regarding the inelastic differential cross section.

(i) The cross section is highly peaked at 0° and the height of the peak further increases with higher values of n. In accordance with the correspondence principle, this nature seems to be quite satisfactory.
(ii) The nature of inelastic differential cross section is controlled by the factor $k_i^2 - k_f^2 = (1/n^2 - 1/n'^2)$.
(iii) If $k_i^2 - k_f^2 > 0.1$ no variation of differential cross section with scattering angle is observed. With the decrease in the value of $k_i^2 - k_f^2$, several local maxima and minima are found to be formed one after another near the forward scattering angle; they slowly move in the forward direction with higher values of n or energy.
(iv) The maxima and minima have been found respectively to be formed due to the constructive and destructive interferences of the scattered waves of different angular momentum states.
(v) The formation of second global maximum in a very short range of scattering angles resembles resonance charateristic of the differential cross section.
(vi) All major variations in the differential cross section are observed for the scattering angle in the range 0°–10° for higher order transitions.

3.2 Total cross section

In Table 4 we present our results for total inelastic cross section for different transitions. These results are fairly accurate as we have already compared our results of total cross section for $1s - 2s$ transition with other available results in the literature [5, 7–10] in our previous paper [1] and have seen that our results for total cross section were in nice agreement with those results.

From Table 4 it is evident that total cross section, as a function of energy, decreases monotonically with energy for all transitions from the $1s$, $2s$ and $3s$ states to any higher states. But for the transitions from ns ($n = 4, 5, 6, ...$) to $n's$ $(5, 6, 7, ...)$, the total cross section as a function of energy presents some deviating feature. Variation in the total cross section with energy is observed for such transitions. Though the variation initially takes place at higher energy region for a transition from 4s state, with the higher values of n such variation gradually shifts towards the lower energy region and becomes more transparent as evident from the Figures 4a–4c.

4 Conclusion

The distorted-wave theory has quite conveniently and elegantly been used to study the $e^+ + \mathrm{H}(ns) \rightarrow e^+ + \mathrm{H}(n's)$ transitions for arbitrary n and n'. Using simple mathematical tools we have quite easily calculated the distorted-wave scattering amplitudes for all significant partial-waves for arbitrary transitions in closed analytical forms. We report results for the differential and total cross sections for arbitrary inelastic $s-s$ transitions. These results are fairly accurate in intermediate and high energy range. Further sufficient analytical and numerical evidences have been presented for the sake of further theoretical and experimental works in this field.

The study of inelastic differential cross section for positron-hydrogen collisions for higher order transition has revealed some hitherto unknown informations. We have found the resonance-like charateristic in the inelastic differential cross section. Further, it has been found that the total cross section for higher order transitions have some deviating features from those of lower order transitions.

References

1. A. Ghoshal, P. Mandal, Phys. Rev. A **72**, 032714 (2005)
2. J. Colgan, D.M. Mitnik, M.S. Pindzola, Phys. Rev. A **63**, 012712 (2000)
3. A.A. Kernoghan, D.J.R. Robinson, M.T. McAlinden, H.R.J. Walters, J. Phys. B **29**, 2089 (1996)
4. V.E. Bubelev, D. Madison, J. Phys. B **25**, 3229 (1992)
5. M. Mukherjee, M. Basu, A.S. Ghosh, J. Phys. B **23**, 757 (1990)
6. C.J. Joachain, R.M. Potvliege, Phys. Rev. A **38**, 4337 (1988)
7. H.R.J. Walters, J. Phys. B **21**, 1893 (1988)
8. B.H. Bransden, I.E. McCarthy, A.T. Stelbovics, J. Phys. B **18**, 823 (1985)
9. L.A. Morgan, J. Phys. B **15**, L25 (1982)
10. F.W. Byron Jr, C.J. Joachain, R.M. Potvlieege, J. Phys. B **14**, L609 (1981)
11. H.S.W. Massey, C.B.O. Mohr, Proc. R. Soc. **A152**, 605 (1931)
12. P.K. Roy, B.C. Saha, N.C. Sil, J. Phys. B **13**, 3401 (1980); P.K. Roy, B.C. Saha, N.C. Sil, J. Phys. B **14**, 2459 (1981)
13. B.C. Saha, N.C. Sil, Phys. Lett. A **87**, 341 (1982)
14. N.C. Sil, B.C. Sil, H.P. Saha, P. Mandal, Phys. Rev. A **19**, 655 (1979)
15. B.H. Bransden, C.J. Joachain *Physics of Atoms and Molecules*, 2nd edn. (Pearson Education, Singapore, 2004), p. 987
16. A. Ghoshal, P. Mandal Phys. Rev. A **72**, 042710 (2005)
17. P. Mandal, S. Kar, U. Roy, Nucl. Inst. Meth. Phys. Res. B **143**, 32 (1998); P. Mandal, S. Kar, U. Roy, Ind. J. Phys. B **73**, 215 (1999)
18. U. Buck, Adv. Chem. Phys. **30**, 313 (1975)
19. M. Tabor, J. Phys. B **10**, 2649 (1977)
20. S. Bosanac, Mol. Phys. **36**, 453 (1978)
21. S. Bosanac, Phys. Rev. A **19**, 125 (1979)
22. A. Schutte, D. Bassi, F. Tommasini, G. Scoles, J. Chem. Phys. **62**, 600 (1975)
23. J.P. Toennies, W. Welz, G. Wolf, J. Chem. Phys. **64**, 5305 (1976)
24. S. Bosanac, Mol. Phys. **35**, 1057 (1978)